A Functional Model for Carbonic Anhydrase: Thermodynamic and Kinetic Study of a Tetraazacyclododecane Complex of Zinc(II)

Xiaoping Zhang[†] and Rudi van Eldik*

Institute for Inorganic Chemistry, University of Erlangen-Nürnberg, Egerlandstrasse 1, 91058 Erlangen, Germany

Received May 12, 1995[⊗]

The hydration of CO_2 and dehydration of HCO_3^- catalyzed by a Zn(II) complex of the macrocyclic tetraamine 1,4,7,10-tetraazacyclododecane ([12]aneN$_4$, cyclen) (**2**) were studied in aqueous solution as a functional model for the zinc-containing carbonic anhydrase. The hydration of CO_2 by **2** yielding protons and bicarbonate ions is a second-order reaction. The rate constant, k^h_{cat}, is (3.3 ± 0.1) × 10^3 $M^{-1}s^{-1}$ at 25 °C and 0.10 M ($NaClO_4$) ionic strength. A plot of hydration rate vs pH (6.0 −9.0) gives a sigmoidal curve with an inflection point at pH 8.1, which is identical to the pK_a value for the Zn(II)-bound water of [cyclen−Zn−H_2O]$^{2+}$ (**2a**). Thus, [cyclen−Zn−OH]$^+$ (**2b**) must play a crucial role in the hydration of CO_2. The catalytic activity of **2b** is the highest of all studied model complexes and reaches almost one-third of the activity of the carbonic anhydrase variant III. The catalyzed dehydration of HCO_3^- by **2a** is also a second-order reaction. The rate constant, k^d_{cat}, is (51 ± 8) $M^{-1}s^{-1}$ at 25 °C and 0.10 M ($NaClO_4$) ionic strength, which exceeds all data reported for other model complexes. The active species for the dehydration of HCO_3^- is [cyclen−Zn−H_2O]$^{2+}$(**2a**). Monovalent anions inhibit competitively the dehydration of HCO_3^- by substituting the coordinated H_2O (inhibition order is $Cl^- < Br^- < I^- < NO_3^-$). A comparison of the structure and activity of 2 with those of (1,5,9-triazacyclododecane)zinc(II) (**4**) leads to the suggestion that the formation of a bidentate bicarbonate intermediate inhibits the catalytic activity. A unidentate bicarbonate intermediate is most likely to be the active species in the carbonic anhydrase catalyzed reaction.

Introduction

Carbonic anhydrases are a family of enzymes found in animals, plants, and bacteria, with the essential physiological function to catalyze the reversible hydration of carbon dioxide according to (1).[1] There are now thought to be at least seven

$$CO_2 + H_2O \rightleftharpoons HCO_3^- + H^+ \qquad (1)$$

human carbonic anhydrases (HCA), of which three have high turnover numbers (10^4 and 10^6),[2] and therefore the nature of the active site has been a topic of great interest.[1] The structure of HCA II in its zinc−water, zinc−hydroxide, and zinc−bicarbonate forms has been characterized in great detail.[3−5] Detailed discussions of the active site in HCA II[1f,3−7] reveal the following key features. The zinc atom is located at the bottom of a conical cavity where it is coordinated by the N atoms of His 94, 96, and 119 and by a water/hydroxide molecule in a slightly distorted tetrahedral geometry (Chart 1). The coordinated water molecule ionizes to a coordinated hydroxide around neutral pH.[8] The enzyme site can be divided into hydrophobic and hydrophilic halves. The hydrophilic half contains the proton acceptor group His 64 and partially ordered water molecules. The inner water environment is almost completely separated from the outer channel by a ring of residues including His 64, His 67, Phe 91, Glu 92, and His 200. Therefore the inner water molecules are not in contact with those which are outside the active site. His 64 bridges those two solvent areas. In the hydrophobic half, a "deep" water molecule, which is thought to be displaced by CO_2 during substrate binding, is found about 3.2 Å from the zinc center. Many hydrophilic residues, together with some water molecules, are involved in a large hydrogen-bonding network.

The most widely accepted catalytic cycle for HCA II is the so-called zinc−hydroxide mechanism.[1] The catalytic activity is characterized by a pK_a value of ca. 7, such that hydration of CO_2 is dominant above pH 7, while dehydration of HCO_3^- is observed below pH 7. It has been postulated that this pK_a value represents that of the coordinated water molecule on the Zn(II) center. A crucial step in the proposed catalytic sequence is the formation of the bicarbonate complex, for which two mechanisms, generally referred to as Lipscomb[9] and Lindskog[10] mechanisms (Scheme 1), have been proposed. In the former

* Address correspondence to this author.
[†] On leave from the Institute of Molecular Science, Shanxi University, Taiyuan, Shanxi, 030006, P. R. China.
[⊗] Abstract published in *Advance ACS Abstracts,* September 15, 1995.

(1) CA has been extensively reviewed: (a) Dodgson, S. J.; Tashian, R. E.; Gros, G.; Carter, N. D. *The Carbonic Anhydrases*. Plenum Press: New York, 1991. (b) Christianson, D. W. *Adv. Protein Chem.* **1991**, *41*, 281−355. (c) Silverman, D. N.; Lindskog, S. *Acc. Chem. Res.* **1988**, *21*, 30. (d) Coleman, J. E. In *Zinc Enzymes*; Bertini, I., Luchinat, C., Maret, W., Zeppezauer, M., Eds.; Birkhäuser: Boston, 1986; p 317. (e) Botré, F.; Gros, G.; Storey, B. T. *Carbonic Anhydrase*; VCH: Weinheim, Germany, 1991. (f) Bertini, I.; Mangani, S.; Pierattelli, R.; *International Conference on Carbon Dioxide Utilization: Lectures and Posters*; University of Bari: Bari, Italy, 1993; p 223.
(2) Merz, K.; Murcko, M. A.; Kollman, P. A. *J. Am. Chem. Soc.* **1991**, *113*, 4484.
(3) (a) Hakansson, K.; Carlsson, M.; Svensson, A.; Liljas, A. *J. Mol. Biol.* **1992**, *227*, 1192. (b) Eriksson, A. E.; Jones, A. T.; Liljas, A. *Proteins* **1988**, *4*, 274.
(4) Nair, S. K.; Christianson, D. *J. Am. Chem. Soc.* **1991**, *113*, 9455.
(5) Xue, Y.; Vidgren, J.; Svensson, L. A.; Liljas, A.; Jonsson, B.-H.; Lindskog, S. *Proteins* **1993**, *15*, 80.
(6) Sola, M.; Lledos, A.; Duran, M.; Betran, J. *J. Am. Chem. Soc.* **1992**, *114*, 869.
(7) Zheng, Y.-J.; Merz, K. M. *J. Am. Chem. Soc.* **1992**, *114*, 10498.
(8) Bertini, I.; Luchinat, C.; Scozzafava, A. *Struct. Bonding* **1982**, *48*, 45.
(9) Lipscomb, W. N. *Annu. Rev. Biochem.* **1983**, *52*, 17.
(10) Lindskog, S. In *Zinc Enzymes*; Spiro, T. G., Ed.; Wiley: New York, 1983; p 77.

0020-1669/95/1334-5606$09.00/0

Chart 1

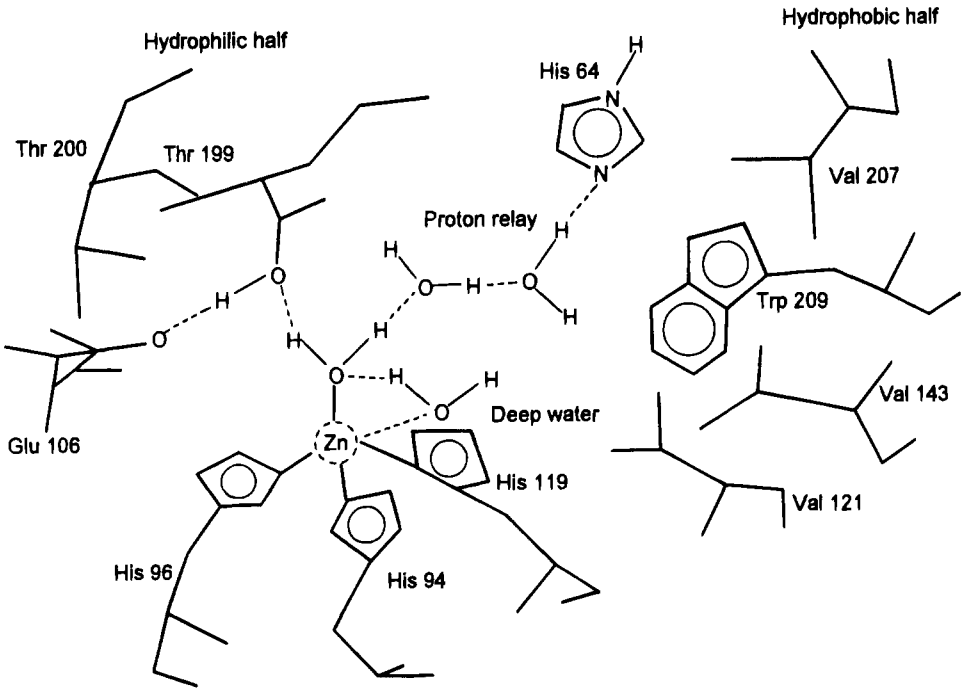

Scheme 1

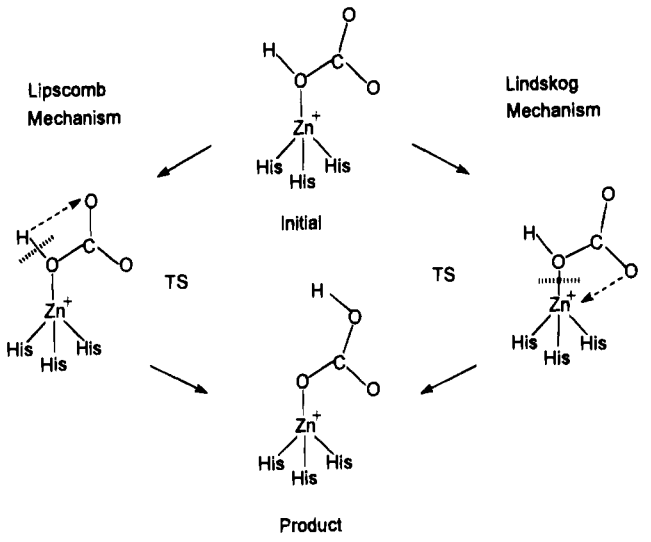

there is proton transfer between two oxygens on the carbonate ligand of the tetrahedral complex, whereas in the latter there is no proton transfer but rather oxygen exchange on the Zn(II) center via a five-coordinate transition state. There is still great controversy concerning the coordination mode of the bicarbonate intermediate. Recent theoretical calculations[7] favor the Lindskog mechanism. The X-ray structure of the bicarbonate complex of the Thr-200 → His mutant of HCA II[5] indicates that the bicarbonate ligand is coordinated to zinc in an asymmetric way with nonequivalent Zn−O bond lengths of 2.2 and 2.5 Å. The protonated oxygen was found to donate a hydrogen bond to Thr 199. This structure is consistent with the equilibrium between four- and five-coordinate species and favors the Lindskog mechanism. A study of the decarboxylation of *cis*-[Cr(cycb)F(OCOOH)]$^+$ suggested that the rate-determining step is proton transfer from an uncoordinated oxygen atom to the coordinated oxygen atom of the bicarbonate ligand,[11] which is in line with the Lipscomb mechanism.

Many studies in recent years have focused on model complexes of Zn(II) to improve the understanding of the structure−reactivity relationship of the active site in HCA.[12-29] In some of the model complexes the chelating ligands have been selected to bind to three coordination sites of Zn(II) via N donor atoms, with the fourth site being occupied by water, hydroxide, or bicarbonate (see Chart 2). In two cases, tetradentate ligands have been employed with the fifth coordination site occupied by water or hydroxide. Complexes **1**, **2a**, **3**, and **4a** in Chart 2 generate L−Zn(II)−OH$^-$ species in solution and the quoted pK_a values are rather close to that for HCA. Although some of the model complexes exhibit a high binding rate for CO_2,[15] they failed to mimic the characteristic pH profile for the catalytic activity of HCA. For many of the model complexes that bind CO_2, no kinetic data have been measured, which complicates

(11) Eriksen, J.; Mønsted, L.; Mønsted, O. *Acta Chem. Scand.* **1992**, *46*, 521.
(12) Marcel, L. M. P.; David, N. R. *J. Am. Chem. Soc.* **1980**, *102*, 7571.
(13) Brown, R. S.; Curtis, N. J.; Huguet, J. *J. Am. Chem. Soc.* **1981**, *103*, 6953.
(14) Brown, R. S.; Salmon, D.; Curtis, N. J.; Kusuma, S. *J. Am. Chem. Soc.* **1982**, *104*, 3188.
(15) Slebocka-Tilk, H.; Cocho, J. L.; Frakman, Z.; Brown, R. S. *J. Am. Chem. Soc.* **1984**, *106*, 2421.
(16) Gellman, S. H.; Petter, R.; Breslow, R. *J. Am. Chem. Soc.* **1986**, *108*, 2388.
(17) Norman, P. R. *Inorg. Chim. Acta* **1987**, *130*, 1. Norman, P. R.; Tate, A.; Rich, P. *Inorg. Chim. Acta* **1988**, *145*, 211.
(18) Iverson, B. L.; Lerner, R. A. *Science* **1989**, *243*, 1185.
(19) Kimura, E.; Shiota, T.; Koike, T.; Shiro, M.; Kodama, M. *J. Am. Chem. Soc.* **1990**, *112*, 5805.
(20) Koike, T.; Kimura, E. *J. Am. Chem. Soc.* **1991**, *113*, 8935.
(21) Kimura, E.; Koike, T. *Comments Inorg. Chem.* **1991**, *11*, 285.
(22) Koike, T.; Kimura, E.; Nakamura, I.; Hashimoto, Y.; Shiro, M. *J. Am. Chem. Soc.* **1992**, *114*, 7338.
(23) Kimura, E. *Pure Appl. Chem.* **1993**, *65*, 355.
(24) Alsfasser, R.; Trofimenko, S.; Looney, A.; Parkin, G.; Vahrenkamp, H. *Inorg. Chem.* **1991**, *30*, 4098.
(25) Alsfasser, R.; Powell, A. K.; Trofimenko, S.; Vahrenkamp, H. *Chem. Ber.* **1993**, *126*, 685.
(26) Alsfasser, R.; Ruf, M.; Trofimenko, S.; Vahrenkamp, H. *Chem. Ber.* **1993**, *126*, 703.
(27) Looney, A.; Han, R.; McNeill, K.; Parkin, G. *J. Am. Chem. Soc.* **1993**, *115*, 4690.
(28) Kitajima, N.; Hikichi, S.; Tanaka, M.; Moro-oka, Y. *J. Am. Chem. Soc.* **1993**, *115*, 5496.
(29) Zhang, X.; van Eldik, R.; Koike, T.; Kimura, E. *Inorg. Chem.* **1993**, *32*, 5749.

Chart 2

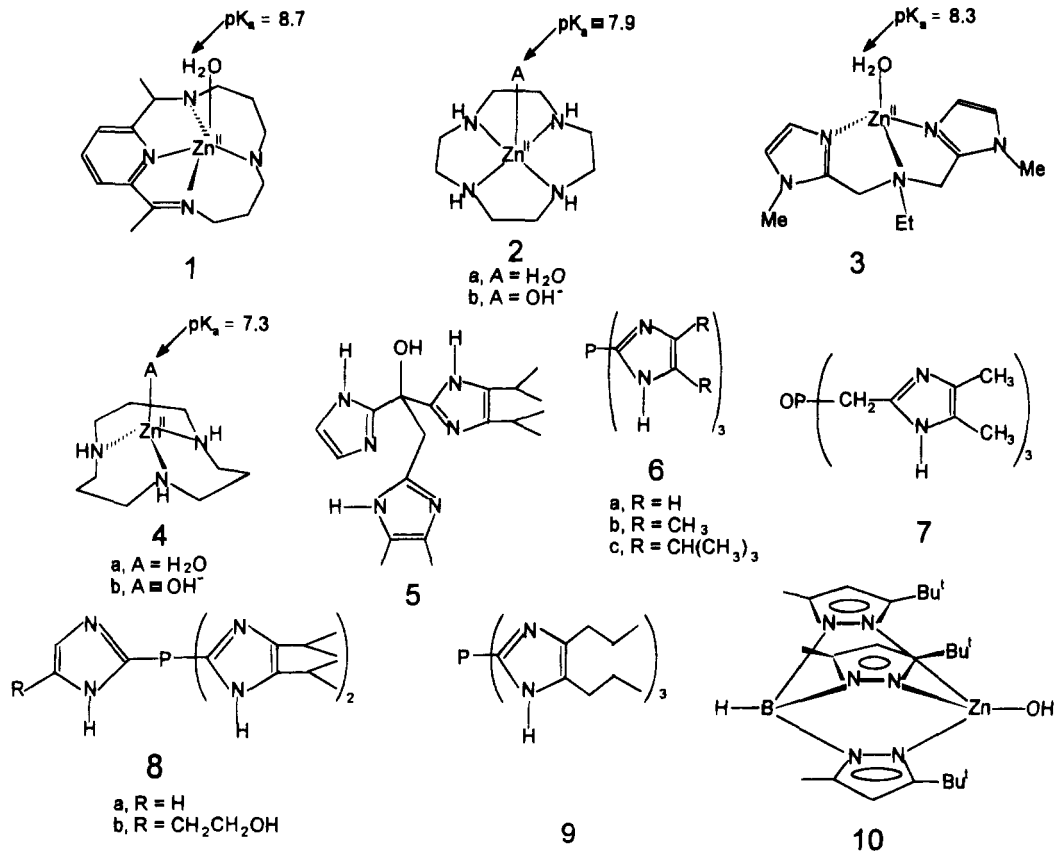

the interpretation of the structure–reactivity relationship In the case of complex **10**, it could be shown that it catalyzes oxygen exchange between CO_2 and $H_2{}^{17}O$.[27] Up to now, complex **4** appears to be the best model available for HCA in terms of its structural, thermodynamic, and kinetic properties.[29] This complex can mimic the catalytic activity of HCA for both the hydration of CO_2 and dehydration of HCO_3^- rather nicely, although its catalytic activity is only moderate compared to that of HCA II.[29]

With respect to the coordination mode of the bicarbonate intermediate and the fundamental difference between the Lipscomb and Lindskog mechanisms (Scheme 1), it is essential to extend our earlier work on complex **4** to complex **2**, where tetraazacyclododecane[12]aneN$_4$ (cyclen), binds four coordination sites of Zn(II). Model **2** is not expected to allow the bidentate coordination of bicarbonate or the exchange of the donor O atom according to the Lindskog mechanism. Furthermore, the pK_a value of 8.0[15] is slightly higher than that for complex **4**, but still reasonably close to that for HCA. Thus a comparative study of models **2** and **4** can provide information on the importance of the coordination mode of the Zn(II) center. We therefore performed a detailed study of the catalytic activity of complex **2** with respect to the hydration of CO_2 and dehydration of HCO_3^- along the lines of our earlier investigation for complex **4**.[27] The goal was to comment on the influence of the coordination geometry of the Zn(II) center on its catalytic acitivity.

Experimental Section

Materials. All reagents used were of analytical reagent grade. The following indicators and biological buffers were purchased and used without further purification: chlorophenol red (Sigma), 4-nitrophenol (Merck), phenol red (Merck), *m*-cresol purple (Sigma), thymol blue (Merck), Mes (2-morpholinoethanesulfonic acid, Merck), Bis-tris ([bis-(2′-hydroxyethyl)amino]tris(hydroxymethyl)methane, Sigma), Mopso (3-morpholino-2–hydroxypropanesulfonic acid, Sigma), Mops (3-morpholinopropanesulfonic acid, Sigma), Hepes (*N*-(2-(hydroxyethyl)-piperazine-N′-ethanesulfonic acid, Merck), Hepps (*N*-(2-hydroxyethyl)-piperazine-N′-propanesulfonic acid, Merck), Taps (3-[(tris(hydroxymethyl)methyl)amino]propanesulfonic acid, Sigma), Ampso (3-[(1,1-dimethyl-2-hydroxyethyl)amino]-2-hydroxypropanesulfonic acid, Sigma). CO_2 (> 99.995%) was purchased from Messer-Griesheim. All solutions were prepared using Milli-pore water which was boiled for more than an hour prior to use to remove the dissolved CO_2.

Preparation of Complex 2: [[12]aneN$_4$–Zn(II)–OH$_2$](ClO$_4$)$_2$. The procedure for the preparation of complex **2** is similar to the method described elsewhere.[17] To a solution of [12]aneN$_4$ (150 mg, 0.87 mmol) in 5 mL of 99.5% EtOH was slowly added, during 1.5 h, a solution of Zn(ClO$_4$)$_2$·6H$_2$O (325 mg, 0.87 mmol) in 5 mL of EtOH at 50–60 °C. After the mixture cooled to room temperature, the white precipitate was filtered off, washed several times with ethanol, and dried for 24 h over CaCl$_2$. Yield: 97 mg (24%). Anal. Found (calcd) for C$_8$H$_{20}$N$_4$Zn(ClO$_4$)$_2$·H$_2$O: C, 21.5 (21.1); H, 4.93 (4.84); N, 12.3 (12.3).

Preparation of CO_2 and HCO_3^- Solutions. A saturated CO_2 solution was prepared by bubbling CO_2 gas into water in a vessel maintained at 25.0 °C. The CO_2 was bubbled for at least 0.5 h before the experiment began, and the bubbling was continued as long as the solution was in use. Dilutions were done by coupling two gastight Hamilton syringes of the Luer type to obtain the required volumes, which were then gently mixed by pushing the contents back and forth between two syringes as described elsewhere.[30] CO_2 concentrations were calculated on the basis of a saturated concentration in water at 25.0 °C of 33.8 mM.[31] The concentration of the saturated CO_2 solution was checked by back-titration with standardized barium hydroxide and standardized HCl using an automatic titrator (Titrino 702 SM) coupled to a Metrohm electrode.

The HCO_3^- solutions were freshly prepared by dissolving $NaHCO_3$ crystals and used within 5 h.

(30) Khalifah, R. G. *J. Biol. Chem.* **1971**, *246*, 2561.
(31) Pocker, Y.; Bjorquist, D. W. *Biochemistry* **1977**, *16*, 5698.

Equilibrium Constant Determinations. Solutions of 1:1 ($c_L = 1.00 \times 10^{-3}$, $c_H = 3.00 \times 10^{-3}$ M) ratio for the ligand, 1:3:1 ratio for the synthetic mixture ($c_L = 1.00 \times 10^{-3}$, $c_H = 3.00 \times 10^{-3}$, $c_M = 1.00 \times 10^{-3}$ M), and 1:3 ratio for back-titration ($c_L = 1.00 \times 10^{-3}$, $c_{ML} = 3.00 \times 10^{-3}$ M) were titrated with a carbonate-free aqueous solution of 0.014 91 M NaOH. The ionic strength was adjusted to 0.10 M by addition of $NaClO_4$. Two titrations were conducted for each system. At least 1.5 h was required to reach equilibration at each point in the titration curve. The electrode response was standardized with buffer solutions at pH 4.01 and 6.86 (25.0 °C). Humidified nitrogen gas free of carbon dioxide (through 1 N NaOH solution) was passed over the solution during the potentiometric measurements. The titrations were carried out at 25.0 ± 0.1 °C. The stability constants of the complexes and the protonation constants of cyclen were obtained by spontaneous optimization using the program MINIQUARD 75.[32] A pK_w for water obtained under the same conditions of 13.94 was used. In order to check for possible polymerization of **2**, six titrations with complex concentrations between 4.5×10^{-4} and 1.0×10^{-2} M were performed under the same conditions.

Kinetic Procedures. All kinetic measurements were performed at 25.0 ± 0.1 °C on a Durrum D110 stopped-flow instrument attached to an on-line data acquisition and handling system, using the OLIS KINFIT (Bogart, GA) set of programs. A Metrohm 632 pH meter equipped with an Ingold V402-S7/120 electrode was connected directly to the receiver reservoir of the stopped-flow instrument in order to determine the pH of the reaction mixture directly after mixing. The reactions were followed using the "pH indicator technique", in which pairs of buffers and indicators having nearly the same pK_a values are employed as described before.[29] Information on the pK_a values, appropriate wavelengths to study the reaction, and the change in extinction coefficient for the selected indicator–buffer pairs has been summarized before.[29] Buffer concentrations were selected in such a way that the total buffer concentration was 50 mM after mixing in the stopped-flow instrument.

The initial rate was estimated from eq 2, where A_o and A_e are the initial and final absorbance values and Q is the buffer factor for converting changes in the absorbance of the indicator to changes in

$$V_{initial} = Q(A_0 - A_e)[d(\ln(A - A_e))/dt]_{t \to 0} \quad (2)$$

CO_2 or HCO_3^- concentration. The value of Q was routinely measured after each kinetic experiment. The value of $[d(\ln(A - A_e))/dt]_{t \to 0}$ was determined by fitting the kinetic trace with a single-exponential fit routine in which the first 10% of the trace was used to calculate the initial rate.

The procedure for a typical kinetic experiment was as follows. One syringe in the stopped-flow apparatus was filled with a 100 mM buffer solution containing $(0-1.25) \times 10^{-3}$ M complex **2**, 0.2 M $NaClO_4$, and ca. 4×10^{-5} M indicator. The second syringe was filled with the freshly prepared CO_2 solution. The concentration of CO_2 was chosen in such a way that it is at least 10 times higher than the complex concentration for the CO_2 hydration reaction. The second syringe was filled with a 0.01 M $NaHCO_3$ solution for the dehydration reaction. The absorbance–time trace was recorded and evaluated as described above. Plots of $V_{initial}$ versus $[Zn(II)]_T$ at a given pH gave good straight lines, from which the slope was used to calculate the second-order rate constant $(k^h_{cat})_{obs}$ or $(k^d_{cat})_{obs}$ for the catalyzed hydration of CO_2 or dehydration of HCO_3^-, respectively, and the intercept was used to calculate the first-order rate constant k^h_{obs} or k^d_{obs} for the spontaneous hydration of CO_2 or dehydration of HCO_3^-, respectively.

Results

Protonation and Complex-Formation Constants. The titration curves are shown in Figure 1. For titration of the ligand (Figure 1a), the inflection occurred at 1 equiv of base. It is due to the free acid present in solution. Thus it follows that two hydrogen atoms are bound to the ligand. Protonation constants of the ligand are log $K_1^H = 11.15 \pm 0.09$ and log $K_2^H = 9.42 \pm 0.04$. They agree well with previous values

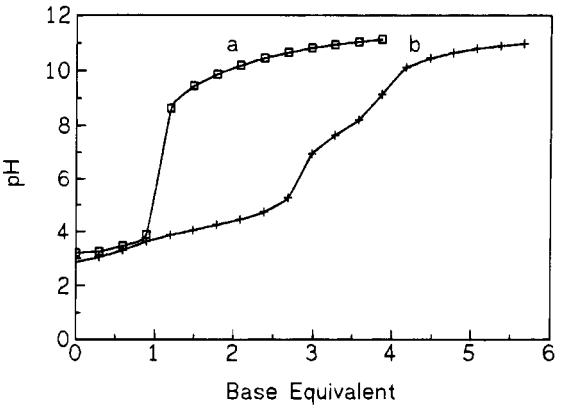

Figure 1. Titration curves for the Zn(II)–[12]aneN$_4$ system at 25 °C and 0.1 M ($NaClO_4$) ionic strength. (a) $c_L = 1.0 \times 10^{-3}$ M, $c_H = 3.0 \times 10^{-3}$ M; (b) (a) + $c_M = 1.0 \times 10^{-3}$ M.

(10.97 and 9.89, respectively[33]). For the titration of the synthetic mixture (Figure 1b), the inflections occur at 1 and 3 equiv of base. The first is due to the free acid present in solution, and the second must be caused by the spontaneously released protons during the formation of $ZnL(H_2O)^{2+}$. The inflection at 4 equiv of base is obviously due to the deprotonation of coordinated water, i.e., the formation of the $ZnLOH^+$ species. Similar results were found for the back-titration of the acidified complex (c_{ML}:c_H = 1:3) compared to those for the titration of synthetic mixture (c_L:c_M:c_H = 1:1:3). The complex-formation constants log K_{ZnL} of 23.5 ± 0.5 and log K_{ZnLOH} of 15.7 ± 0.6 were obtained, as well as a pK_a for $ZnL(H_2O)^{2+}$ of 7.9 ± 0.2. The pK_a value agrees with the value of 8.0 at 1 M ionic strength reported elsewhere.[17] The complex formation and acid–base equilibria involved during titration are defined by eqs 3–6. On the basis of these equations and the values of

$$H^+ + L = HL^+$$

$$K_1^H = \frac{[HL^+]}{[H^+][L]} = 10^{11.15 \pm 0.09} \quad (3)$$

$$H^+ + HL^+ = H_2L^{2+}$$

$$K_2^H = \frac{[H_2L^{2+}]}{[H^+][HL^+]} = 10^{9.42 \pm 0.04} \quad (4)$$

$$Zn(H_2O)^{2+} + L = ZnL(H_2O)^{2+}$$

$$K_{ZnL} = \frac{[ZnL(H_2O)^{2+}]}{[Zn(H_2O)^{2+}][L]} = 10^{23.5 \pm 0.5} \quad (5)$$

$$ZnL(H_2O)^{2+} = ZnLOH^+ + H^+$$

$$K_a = \frac{[ZnLOH^+][H^+]}{[ZnL(H_2O)^{2+}]} = 10^{-(7.9 \pm 0.2)} \quad (6)$$

K_1^H, K_2^H, K_{ZnL}, and K_a, the distribution curves for the various species in solution can be calculated, and the results are summarized in Figure 2. It follows that the formation of ZnL-

(32) Gans, P.; Sabatini, A.; Vacca, A. *Inorg. Chim. Acta* **1976**, *18*, 237.

(33) Leugger, A. P.; Hertli, L.; Kaden, T. A. *Helv. Chim. Acta* **1978**, *61*, 2295 and references therein.

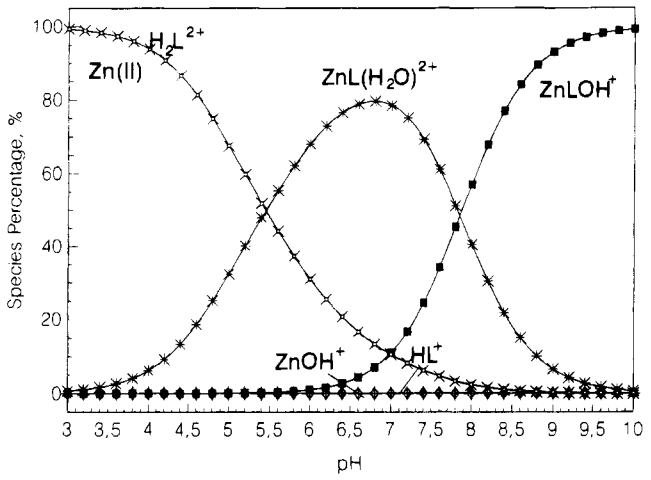

Figure 2. Distribution curves for the [12]aneN$_4$ system as a function of pH. Experimental conditions: temp = 25 °C; ionic strength = 0.10 M ($NaClO_4$).

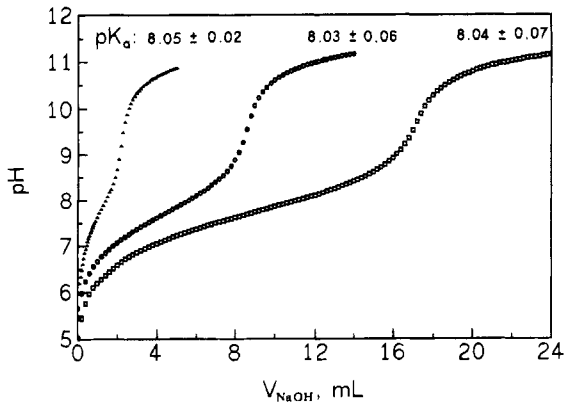

Figure 3. Titration curves for different concentrations of complex **2**: (△) [**2**] = 0.45 mM, [H^+] = 0.1002 mM, [NaOH] = 8.006 mM; (○) [**2**] = 5.00 mM, [H^+] = 0.1002 mM, [NaOH] = 9.911 mM; (□) [**2**] = 10.0 mM, [H^+] = 0.2003 mM, [NaOH] = 9.911 mM; Experimental conditions: temp = 25 °C; ionic strength = 0.10 M ($NaClO_4$); volume of complex solution titrated = 15 mL.

$(H_2O)^{2+}$ starts at a pH of 4 and this is the main species around a pH of 6.1−7.2. At a pH of 7.1, the coordinated water of $ZnL(H_2O)^{2+}$ starts to deprotonate to form $ZnLOH^+$. In a weakly basic medium around a pH of 9, $ZnLOH^+$ is the main species in solution. It was reported in the literature[17] that complex **2** could form a dimer under certain conditions. For this reason a series of titrations were performed for different concentrations of **2** in order to know whether the influence of a dimer on the kinetic data should be considered; three titration curves are shown in Figure 3. The results show that the corresponding pK_a values are independent of the complex concentration, from which it follows that the complex is monomeric in our studied concentration range.

Hydration of CO_2. The kinetics of the uncatalyzed and catalyzed hydration of CO_2 were studied under the same conditions in the pH range 6.1−9.1. The dependence of the initial rate on the concentration of complex **2** is reported in Figure 4 as a function pH, and the results are summarized in Table 1. It follows that the rate of hydration of CO_2 varies linearly with the complex concentration and increases significantly on increasing pH. The results in Table 1 clearly demonstrate the good agreement between the values of k^h_{obs} for the spontaneous hydration reaction measured directly or determined from the intercepts of the plots in Figure 4. The values of $(k^h_{cat})_{obs}$ are plotted as a function of pH in Figure 5. The sigmoid shaped curve is characteristic for such catalytic

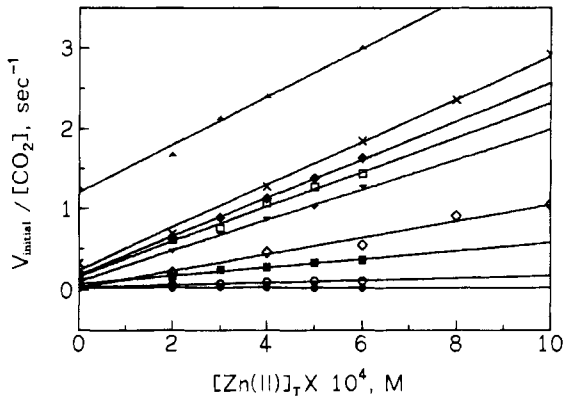

Figure 4. Initial rate/[CO_2] versus [Zn(II)]$_T$ for hydration of CO_2 as a function of pH at 25.0 °C: (●) pH = 6.1; (◇) pH = 7.79; (□) pH = 8.50; (○) pH = 6.86; (▼) pH = 8.22; (×) pH = 8.83; (■) pH = 7.48; (◆) pH = 8.51; (▲) pH = 9.11. Experimental conditions: see Table 1.

processes and similar to that found for model **4**[29] and HCA[1]. This pH dependence can be accounted for in terms of the mechanism outlined in (7), which is based on the principle that

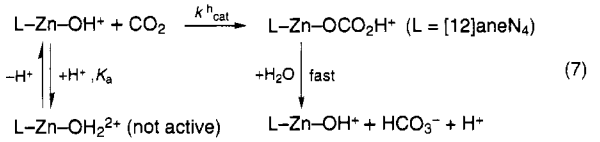

(7)

only the hydroxo complex can catalyze the hydration reaction.[34,35] In this scheme the produced bicarbonate complex is unstable and rapidly aquates to release HCO_3^- and H^+. It is safe to assume that no stable bicarbonate complex is formed since the release of protons is observed during the reaction.

The rate law for the mechanism in (7) is given in (8), from which it follows that a plot of $(k^h_{cat})_{obs} - 1$ versus [H^+] should be linear. This is indeed the case as shown in Figure 6, from

$$(k^h_{cat})_{obs} = k^h_{cat}K_a/([H^+] + K_a) \quad (8)$$

which it follows that $K_a = (7.24 \pm 0.23) \times 10^{-9}$ M and $k^h_{cat} = (3.3 \pm 0.1) \times 10^3$ M^{-1} s^{-1} at 25.0 °C. This pK_a value of 8.1 ± 0.1 is very close to that of 7.9 ± 0.2 determined from the potentiometric titrations reported above. The values of K_a and k^h_{cat} were used to draw the sigmoid curve through the experimental points in Figure 5. It follows that the catalyzed hydration mechanism (8) is in good agreement with the experimental data.

Dehydration of HCO_3^-. The uncatalyzed and catalyzed dehydration reactions were studied under similar conditions in the pH range 5.7−7.0. The reaction could only be studied over this limited pH range due to interference of the reverse hydration reaction at pH > 7.0 and the spontaneous acid-catalyzed dehydration of HCO_3^- at pH < 5.6. Typical plots of initial rate vs [Zn(II)] are shown in Figure 7. The results are summarized in Table 2. The obtained values of $(k^d_{cat})_{obs}$ increase slightly with increasing pH. This trend is similar to the trend in the fraction of the aquo complex (α; see Table 2). It indicates that the aquo complex is the active species. The values of the corrected rate constant, k^d_{cat}, based on the value of α at each measured pH are indistinguishable within the error limits. The mean value of k^d_{cat} is 51 ± 8 M^{-1} s^{-1}. The spontaneous reaction

(34) Palmer, D. A.; van Eldik, R. *Chem. Rev.* **1983**, *83*, 694 and references cited therein.
(35) Chaffee, E.; Dasgupta, T. P.; Harris, G. M. *J. Am. Chem. Soc.* **1973**, *95*, 4147.

Table 1. Summary of Rate Constants for the Uncatalyzed and Catalyzed Hydration Reaction of CO_2[a]

buffer	10^5[indicator], M	pH[b]	$(k^h_{cat})_{obs}$,[c] M^{-1} s^{-1}	k^h_{obs},[d] s^{-1}	k^h_{obs},[e] s^{-1}
Mes	2.83	6.10	0	0.026 ± 0.003	0.026 ± 0.004
Mopso	4.31	6.86	163 ± 13	0.030 ± 0.002	0.026 ± 0.004
Hepes	2.26	7.48	564 ± 26	0.067 ± 0.001	0.04 ± 0.02
Hepps	4.19	7.79	1013 ± 74	0.057 ± 0.006	0.03 ± 0.04
	4.19	8.22	1887 ± 51	0.112 ± 0.026	0.11 ± 0.02
Taps	4.16	8.51	2390 ± 40	0.20 ± 0.03	0.18 ± 0.02
Ampso	2.40	8.50	2154 ± 82	0.17 ± 0.06	0.17 ± 0.03
	2.40	8.83	2649 ± 80	0.333 ± 0.012	0.25 ± 0.05
Ches	2.40	9.11	3012 ± 193	1.27 ± 0.06	1.27 ± 0.07

[a] Experimental conditions: $[buffer]_T$ = 50 mM; temp = 25.0 °C; ionic strength = 0.1 M ($NaClO_4$); $[CO_2]$ = 8.5 × 10^{-4} to 1.12 × 10^{-2} M. [b] Mean pH calculated from pH measurements before and after the reaction. The difference in pH was not more than 0.15 unit at pH < 8.5 and not more than 0.30 unit at pH > 8.8. [c] Observed second-order rate constant, i.e. slope of curves in Figure 4. [d] Data measured directly for the uncatalyzed hydration reaction. [e] Data extrapolated from Figure 4 (i.e. intercepts).

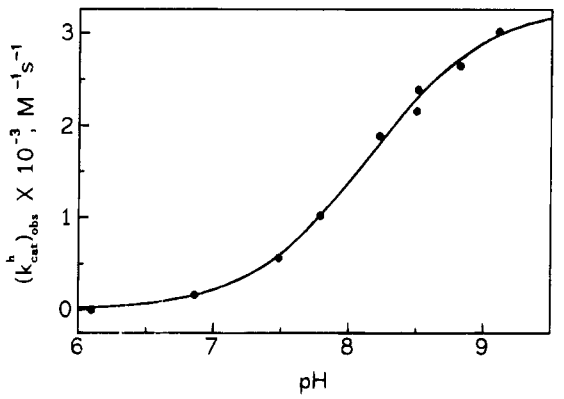

Figure 5. Plot of $(k^h_{cat})_{obs}$ versus pH. For experimental conditions, see Table 1. The solid line was calculated on the basis of the mechanism outlined in eq 7—see Discussion.

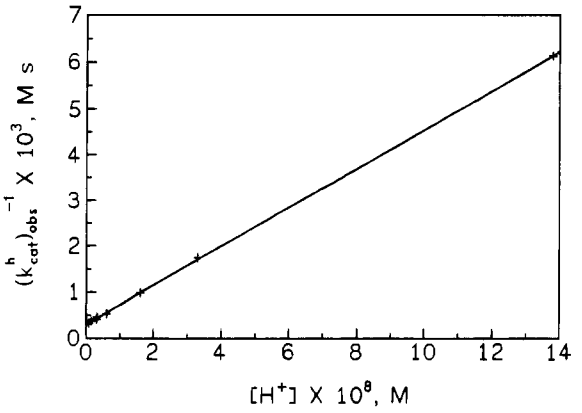

Figure 6. Plot of $(k^h_{cat})_{obs}^{-1}$ versus $[H^+]$ for the data in Table 1.

rate also showed a reasonable decrease with increasing pH. The suggested mechanism is shown in (9).

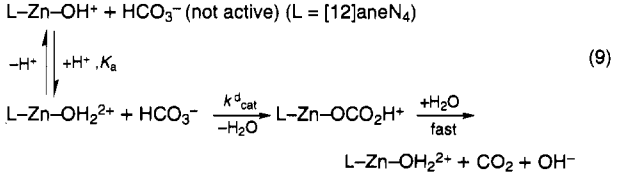

(9)

Effect of Added Monovalent Anions on k^d_{cat}. It has long been recognized that monovalent anions inhibit the activity of HCA.[1,36,37] The results in Table 3 demonstrate that addition of NaCl, NaBr, NaI, and $NaNO_3$ also decreases the catalytic activity of complex **2** during the dehydration of HCO_3^-. The

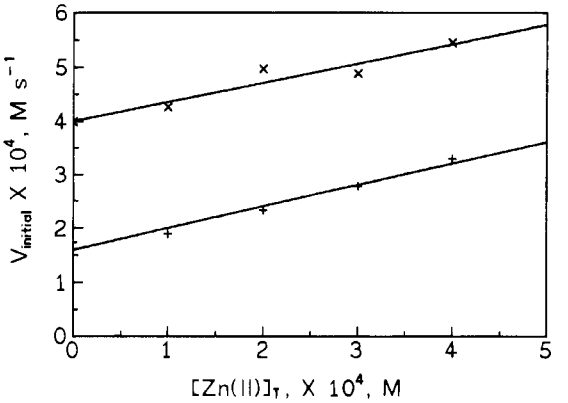

Figure 7. Typical plots of inital rate versus $[Zn(II)]_T$ for the dehydration of HCO_3^-: (×) pH = 6.15; (+) pH = 6.73. Experimental conditions: see Table 2.

Table 2. Summary of Rate Constants for the Uncatalyzed and Catalyzed Dehydration Reaction of HCO_3^- [a]

buffer	pH[b]	pH[c]	$(k^d_{cat})_{obs}$, M^{-1} s^{-1}	α[d]	k^d_{cat},[e] M^{-1} s^{-1}	$10^2V_{initial}/[HCO_3^-]$,[f] s^{-1}
Mes	5.66	5.88	30.5 ± 3.2	0.59	51.7 ± 5.3	9.23 ± 0.24
	6.15	6.39	36.0 ± 6.71	0.71	50.7 ± 8.4	4.05 ± 0.03
	6.30	6.94	36.5 ± 0.1	0.75	49.0 ± 0.13	2.41 ± 0.03
Mopso	6.73	6.87	41.3 ± 3.2	0.80	51.6 ± 4.0	1.73 ± 0.08

[a] Experimental conditions: $[buffer]_T$ = 50 mM; temp = 25.0 °C; ionic strength = 0.1 M. ($NaClO_4$); $[HCO_3^-]$ = 0.01 M. [b] pH of the solution before reaction. [c] pH of the solution after reaction. [d] The fraction of aqua complex, $ZnL(H_2O)^{2+}$, in solution based on Figure 2. [e] Data corrected for the fraction of aqua complex, $k^d_{cat} = (k^d_{cat})_{obs}/\alpha$. [f] Data extrapolated from Figure 7: $V_{inital} = k^d[HCO_3^-][H^+]$[29].

Table 3. Influence of Monovalent Anions on the Value of $(k^d_{cat})_{obs}$[a]

[anion]/[**2**][b]	NaCl	NaBr	NaI	NaNO3
0.0	54.7 ± 2.6			
0.5	48.3 ± 2.1			
1.0	40.8 ± 1.6	46.7 ± 2.4	49.4 ± 2.1	50.2 ± 1.7

[a] Experimental conditions: temp = 25.0 ± 0.2 °C; [**2**] = 5 × 10^{-3} M; $[NaHCO_3]$ = (1−10) × 10^{-3} M; [chlorophenol red] = 1.89 × 10^{-5} M; [Mes] = 5.0 × 10^{-2} M; ionic strength = 0.1 M ($NaClO_4$); pH (before reaction) = 6.17; pH (after reaction) = 6.17−6.30; $(k^d_{cat})_{obs}$ is quoted in M^{-1} s^{-1}. [b] Concentration of added anion divided by the concentration of catalyst **2**.

influence of the anions on the values of $(k^d_{cat})_{obs}$ increases with decreasing size of the anion ($Cl^- < Br^- < I^- < NO_3^-$). This means that the smaller anions can effectively substitute the coordinated water molecule and compete with the rate-determin-

(36) (a) Lindskog, S. *J. Biol. Chem.* **1963**, *238*, 945. (b) Lindskog, S.; Nyman, P. O. *Biochim. Biophys. Acta* **1964**, *85*, 462.

(37) (a) Roughton, F. J. W.; Booth, V. H. *Biochem. J.* **1946**, *40*, 319. (b) Meldrum, N. U.; Roughton, F. J. W. *J. Physiol. (London)* **1933**, *80*, 143. (c) King, R. W.; Burgen, A. S. V. *Proc. R. Soc. London, Ser. B* **1976**, *193*, 107.

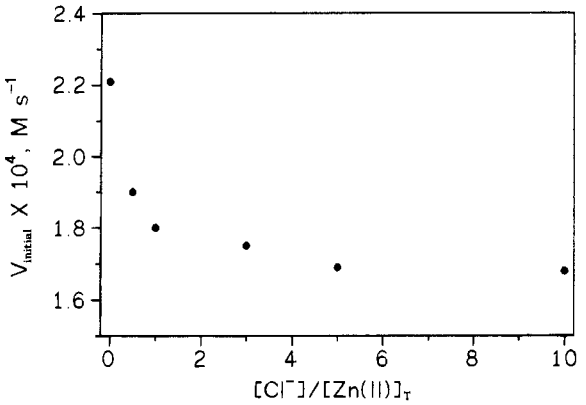

Figure 8. Effect of $[Cl^-]$ on the initial rate for the catalyzed dehydration of HCO_3^-. Experimental conditions: [Mes] = 50 mM; [chlorophenol red] = 1.89 × 10^{-5} M; [**2**] = 1.0 × 10^{-3} M; ionic strength = 0.1 M ($NaClO_4$); pH (before reaction) = 6.0; pH (after reaction) = 6.00−6.17.

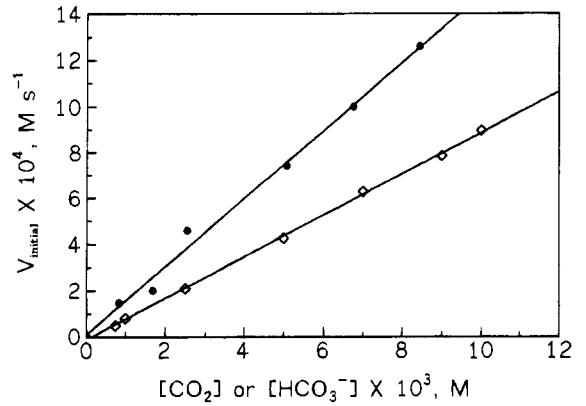

Figure 9. Initial rate for the catalyzed hydration of CO_2 and dehydration of HCO_3^- as a function of $[CO_2]$ and $[HCO_3^-]$, respectively. Experimental conditions (temp = 25.0 ± 0.2 °C): (●) hydration reaction, [Hepes] = 50 mM, [**2**] = 4 × 10^{-4} M, [phenol red] = 2.26 × 10^{-5} M, ionic strength = 0.10 M ($NaClO_4$), pH (before reaction) = 7.59, pH (after reaction) = 7.25−7.50; (◇)dehydration reaction, [Mes] = 50 mM, [**2**] = 1 × 10^{-3} M, [chlorophenol red] = 1.89 × 10^{-5} M, ionic strength = 0.10 M ($NaClO_4$), pH (before reaction) = 6.13, pH (after reaction) = 6.11−6.20

ing coordination of HCO_3^- during the dehydration reaction. The decrease in catalytic activity becomes more marked on increasing the anion concentration as shown for a typical example in Figure 8. Such effects of added anions were not observed for the uncatalyzed dehydration of HCO_3^-.[14]

Observation of Non-Michaelis−Menten Behavior. In other experiments, kinetic evidence for the possible formation of precursor ion-pair or encounter complexes during the catalyzed hydration and dehydration reactions was sought by performing a detailed concentration dependence study. The results in Figure 9 clearly show that the plots of initial rate versus $[CO_2]$ and $[HCO_3^-]$ exhibit no significant curvature within the experimental error limits, i.e. no kinetic evidence for precursor formation.

Discussion

It follows from the above reported data that model **2** exhibits a significant catalytic activity for both hydration of CO_2 and dehydration of HCO_3^-. In neutral or weakly acidic medium, **2a** is the catalytically active species for the dehydration of HCO_3^-. The rate-dertermining step is the substitution of coordinated H_2O by HCO_3^-, followed by the rapid decarboxylation of the bicarbonate complex. In weakly basic solution, the less labile hydroxo complex can bind CO_2 in the rate-determining step, followed by the rapid aquation reaction of the bicarbonate complex. It follows that there is competition between uptake/decarboxylation reactions, on the one hand, during which no Zn−O bond cleavage occurs, and substitution reactions, on the other hand, that do involve Zn−O bond cleavage. Consequently, coordinated bicarbonate can either be substituted by water during the hydration reaction or undergo decarboxylation during the dehydration reaction. This will presumably be controlled by the location of the proton on the bicarbonate ligand, viz. $L-Zn-O(H)CO_2^+$ or $L-Zn-OCO_2H^+$ (see Scheme 1). The overall catalytic cycle is summarized in Scheme 2.

Scheme 2[a]

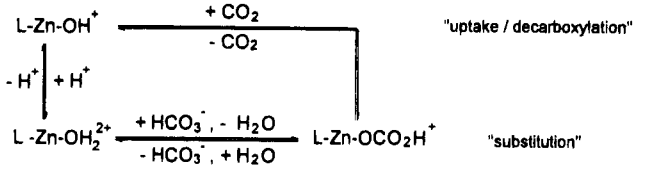

[a] L = [12]aneN$_4$.

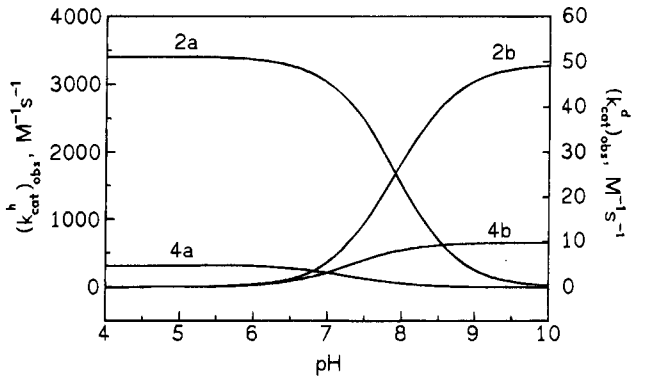

Figure 10. pH profiles for the catalyzed hydration of CO_2 and dehydration of HCO_3^- by complexes **2** and **4** extrapolated from the reported kinetic data at 25 °C and 0.1 M ionic strength.

To what extent does the presently investigated [12]aneN$_4$ complex of Zn(II) serve as a functional model for HCA? There are now two model complexes, **2** and **4**, that excellently mimic the catalytic cycle of HCA-catalyzed CO_2 hydration and HCO_3^- dehydration, although **2** is a five-coordinate and **4** is a four-coordinate species (Chart 2). The pH profiles which clearly demonstrate the catalytic activity of complexes **2** and **4** during the hydration of CO_2 and dehydration of HCO_3^- are summarized in Figure 10. Model **2b** is ca. 5 times more reactive than **4b** for hydration of CO_2, and model **2a** is ca. 11 times more reactive than model **4a** for dehydration of HCO_3^-. Kinetic data for different carbonic anhydrases are summarized in Table 4. For the hydration of CO_2, k^h_{cat} has values between 10^4 and 10^6 s^{-1} (assigned to the proton transfer step[1,38]) and the second-order rate constant k^h_{cat}/K^h_m (assigned to the binding of CO_2[1,38]) varies between 10^5 and 10^8 M^{-1} s^{-1}. On the other hand, the dehydration reactions are characterized by values for k^d_{cat} of 10^5-10^6 s^{-1} (assigned to proton transfer[1] and most probably simultaneous release of CO_2[39]) and for k^d_{cat}/K^d_m of 10^6-10^7

(38) Silverman, D. N.; Lindskog, S. *Acc. Chem. Res.* **1988**, *21*, 30.
(39) Zhang, Z.; Hubbard, C. D.; van Eldik, R. Submitted.
(40) Steiner, H.; Jonsson, B. H.; Lindskog, S. *Eur. J. Biochem.* **1975**, *59*, 253.
(41) Simonsson, L.; Jonsson, B. H.; Lindskog, S. *Eur. J. Biochem.* **1979**, *93*, 409.
(42) Rowlett, R. S.; Silverman, D. N. *J. Am. Chem. Soc.* **1982**, *104*, 6737.
(43) Kogut, K. A.; Rowlett, R. S. *J. Biol. Chem.* **1987**, *262*, 16417.
(44) Kararh, T.; Silverman, D. N. *J. Biol. Chem.* **1985**, *260*, 3484.
(45) Wolley, P. *Nature* **1975**, *258*, 677.

Table 4. Summary of Kinetic Parameters at 25 °C for the Hydration of CO_2 and Dehydration of HCO_3^- Catalyzed by Different Carbonic Anhydrases

enzyme	pK_{E1}[a]	k^h_{cat}, s^{-1}	pK_{E2}[a]	k^h_{cat}/K^h_m, M^{-1} s^{-1}	ref
HCA I	ca. 7	2×10^5		5.0×10^7	30
	ca. 7.1	2.2×10^5		3.14×10^7	1e
HCA II	ca. 6.8	1.4×10^6		1.6×10^8	30
	ca. 6.3	1.0×10^6		1.2×10^8	40
	ca. 6.6	2.5×10^5		1.2×10^8	40b
		3.1×10^5		4.1×10^5	41
		9.0×10^4		1.1×10^5	41b
		8×10^5	7.60	1.0×10^8	42
	6.87	1.06×10^6	7.03	8.7×10^7	43
	6.8	1.0×10^6		1.1×10^8	1e
		8.14×10^5		9.3×10^7	39
Co^{2+}–HCA II	6.58	3.05×10^5	7.23	8.8×10^7	43
HCA III		1.0×10^4		3.0×10^5	44

enzyme	pK_{E1}[a]	k^d_{cat}, s^{-1}	k^d_{cat}/K^d_m, M^{-1} s^{-1}	ref
HCA II	ca. 6.3	6×10^5	1.8×10^7	40
	ca. 6.6	1.6×10^5	1.4×10^7	40b
		4.1×10^5		41
		1.1×10^5		41b
		2.2×10^5	5.8×10^6	44

[a] pK_{E1} and pK_{E2} represent the deprotonation constants for the catalytic site and the proton transfer group, respectively. [b] Measured in D_2O.

Table 5. Summary of Kinetic Data at 25 °C for the Hydration of CO_2 and Dehydration of HCO_3^- Catalyzed by Different Model Complexes[a]

complex	pK_a	k^h_{cat}, M^{-1} s^{-1}	pH	ref
1	8.7	225 ± 23		45
4a	7.3	654 ± 57		29
2a	8.1	3300 ± 100		this work
Zn(**5**)OH^+	*b*	760 ± 50	6.5	12
		240 ± 20	7.5	12
Zn(**6a**)OH^+		no effect		12
Zn(**6b**)OH^+		no effect		12
Zn(**6c**)OH^+		626–898	7.3–6.4[c]	13
		472–900	6.1–7.3[d]	13
Zn(**7**)OH^+	ca. 6	92–156	6.4–7.0	14
Zn(**8a**)OH^+		0–1520	6.2–6.8	15
Zn(**9**)OH^+		1760–2480	6.2–6.8	15
Zn(**10**)OH^+		100–1000		27
M(L)OH^{n+} [e]		44–590		34
$H_2O + CO_2$		$(7.8 \pm 1.2) \times 10^{-4}$		29
$OH^- + CO_2$		$7.9 \pm 0.6) \times 10^3$		29

complex	pK_a	k^d_{cat}, M^{-1} s^{-1}	ref
Zn([12]aneN$_3$)H_2O^{2+}	7.4	4.7 ± 0.6	29
Zn([12]aneN$_4$)H_2O^{2+}	7.9	51 ± 8	this work
M(L)OCO_2H^{n+} [f]	5.6–7.0	0.3–2.9[g]	34
$H^+ + HCO_3^-$		$(5.9 \pm 0.5) \times 10^4$	29

[a] k^h_{cat} for the model complexes of ligands 5–10 represents the sum of the catalytic rate constants ($k^h_{cat} + k^d_{cat}$) for the hydration and dehydration reactions.[12] [b] No typical catalytic pH profile was observed. [c] Determined from hydration reaction. [d] Determined from dehydration reaction. [e] M(L)OH^{n+} represent 22 different transition metal complexes summarized in ref 34, where L represents an amine ligand. [f] The pK_a values in this case are for the deprotonation of the bicarbonate complexes derived from the series of M(L)OH^{n+} complexes. [g] First-order rate constant for the decarboxylation of coordinated bicarbonate.

M^{-1} s^{-1}. It is surprising to note that the five-coordinate model **2** has such a high activity, almost one-third of that of HCA III. The rate constants for other model complexes are summarized in Table 5, which demonstrates that **2b** exhibits the highest catalytic activity of all model complexes for the hydration of CO_2 and **2a** exhibits by far the highest activity of all model complexes for the dehydration of HCO_3^-.

(46) Koike, T.; Kajitani, S.; Nakamura, I.; Kimura, E.; Shiro, M. *J. Am. Chem. Soc.* **1995**, *117*, 1212.

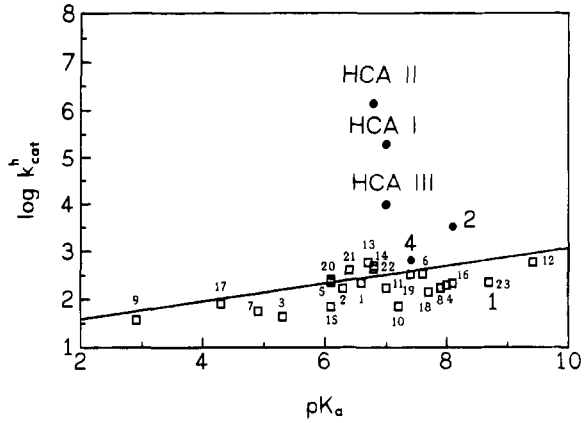

Figure 11. Plot of log k^h_{cat} versus pK_a for the hydration of CO_2 by carbonic anhydrases and a series of model complexes: (□) points and small numbers refer to a series of complexes of the type M(L)OH^{n+} reported in ref 34; (●) points and large numbers refer to the systems in Tables 4 and 5.

Can such a high activity of **2** be accounted for by the pK_a of 7.9 which is slightly higher than that for HCA? We present a correlation between the activity of many model hydroxo complexes toward the binding of CO_2 and the pK_a values of the corresponding aqua complexes in Figure 11. The line through some of the data was taken from an earlier correlation.[34] It shows that the catalytic activity of model complexes increases with increasing pK_a of the coordinated water molecule. Complex **4** studied before[29] fits this correlation quite well, whereas the presently investigated complex **2** shows a marked increase in activity that cannot be related to the small increase in pK_a value. Thus the high activity of **2** cannot only be correlated with the slightly increased pK_a value of 7.9. It is therefore suggested that the low pK_a of around 7 for coordinated water in the active center of the enzyme may not be critical for a high catalytic activity but more likely may be important for a reversible hydration reaction at physiological pH.

Notwithstanding the impressive activity of complex **2**, it is still orders of magnitude below that of HCA I and HCA II. An effective preassociation of CO_2 with the hydrophobic pocket (binding constant of 10^4 M^{-1})[29] could in principle account for the large difference in activity between HCA and the model complexes. In one study,[15] the high catalytic activity of Zn(**9**)OH^+ was assigned to a more hydrophobic environment of the reactive center. The experiments performed in the present study exhibited no curvature in the concentration dependence plots, which is a characteristic of precursor formation steps (see Figure 9). Therefore the high activity of **2** cannot be accounted for by an effective preassociation of CO_2 with **2b** in the hydration reaction and of HCO_3^- with **2a** in the dehydration reaction.

The high activity of models **2a** and **2b** may be related to the stability constants for these complexes. The stability constants for **2a** and **2b** (23.5 and 15.7, respectively) are significantly higher than those for **4a** and **4b** (8.65 and 6.48, respectively) and other model complexes (see Table 6). A high stability constant for the binding of the chelate ligand will result in a more labile coordinated water molecule and a higher nucleophilicity of the coordinated hydroxy ligand. This in turn will favor ligand substitution of water by HCO_3^- and nucleophilic attack of coordinated OH^- on carbon of CO_2. The nucleophilicity of the coordinated hydroxide will control the binding rate of CO_2, whereas the strength of the Zn–O bond in coordinated bicarbonate will control the release of HCO_3^-.

What do these trends mean in terms of the coordination mode around the Zn(II) center in the model complexes? The

Table 6. Summary of Overall Stability Constants for Various Model Zinc Complexes and Carbonic Anhydrase

complex	l	p	q[a]	log β[b]	ref
4a	1	1	0	8.65 ± 0.07	29
4b	1	1	−1	1.11 ± 0.04	29
2a	1	1	0	23.5 ± 0.5	this work
2b	1	1	−1	15.7 ± 0.5	this work
				15.3 ± 0.1	46
$Zn(\mathbf{6c})^{2+}$	1	1	0	6.00 ± 0.04	14
$Zn(\mathbf{7})^{2+}$	1	1	0	6.19 ± 0.03 to 6.67 ± 0.05[c]	14
$Zn(\mathbf{8a})^{2+}$	1	1	0	8.7[d]	15
$Zn(\mathbf{8b})^{2+}$	1	1	0	6.5[d]	15
$Zn(\mathbf{9})^{2+}$	1	1	0	8.0[d]	15
$Zn(enzyme)^{2+}$	1	1	0	10.5[d]	36

[a] l, p, and q are the stoichiometric coefficients corresponding to Zn^{2+}, L, and H^+, respectively. [b] $\beta = [Zn_lL_pH_q]/[Zn]^l[L]^p[H]^q$. [c] Value depends on the contents of EtOH (8−20%). [d] No error limits reported in the literature.

Chart 3

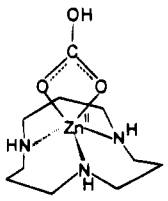

(a) Stronger tendency to form bidentate bicarbonate intermediate for **4**

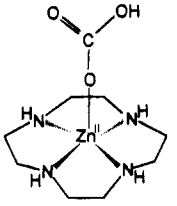

(b) Weaker tendency to form bidentate bicarbonate intermediate for **2**

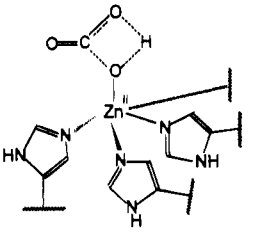

(c) Suggested unidentate bicarbonate intermediate in HCA

significantly higher activity of **2b** than that of **4b** for the hydration of CO_2 must also be related to the fact that it is a five-coordinate species. In general, chelation of coordinated bicarbonate will tend to stabilize the carbonate complex and slow down the overall hydration process.[34] Five-coordinate **2b** has less possibility to form a bidentate bicarbonate complex than the four-coordinate complex **4b** (see Chart 3). In the case of the five-coordinate **2b** complex, chelation of coordinated carbonate is unlikely and will therefore accelerate the release of HCO_3^- and the overall hydration reaction. Although one can never be certain that extrapolations to enzymes made on the basis of model studies are accurate, we do suggest that the coordination mode of Zn(II) in the active center of the enzyme may change during the catalytic cycle by a weak binding to a neighboring group to form a five-coordinate species, such that only a unidentate bicarbonate complex can be formed, which seems to be critical for an efficient catalytic cycle (Chart 3). In the case of Co(II)-substituted HCA, spectral evidence was reported for a four- and five-coordinate metal center depending on the pH of the solutions.[38]

Thus **2** is presently the best model for mimicking the structure of a five-coordinate species of HCA in solution. Recent work on model complexes of type **10**[27] clearly demonstrated that the formation of a bidentate carbonate intermediate inhibits the catalytic cycle during the hydration of CO_2. Furthermore, studies on metal-substituted carbonic anhydrases[1,27] have revealed that the order of activity decreases along the series Zn > Co ≫ Ni and Cu, which correlates with the tendency of these metals to favor a bidentate coordination mode in model systems with nitrate. The fact that the $Zn([12]aneN_4)OCO_2H^+$ complex is a 20-electron species, which causes a labilization of coordinated bicarbonate in order to undergo a dissociative substitution reaction, may also be a reason for the higher activity. Eriksen et al.[11] pointed out that protonation of the coordinated oxygen atom, which is the case immediately following the binding of CO_2, will weaken the metal−oxygen bond and facilitate release of HCO_3^-. It should be noted that the opposite trend was observed for these model complexes during the hydrolysis of organic phosphates.[20] In this case the Zn(II)-bound OH^- acts as a nucleophile and the vacant coordination site anchors the substrate P=O or $P-O^-$ group. Thus **4b** exhibited a significantly higher reactivity than **2b** since it can more easily bind the organic phosphate in a bidentate manner.

The dehydration reaction follows the reactivity sequence **2a** > **4a**. The low reactivity observed for **4a** may once again be related to the possible chelation of coordinated bicarbonate, which will slow down the decarboxylation reaction. The higher reactivity of **2b** can then be ascribed to the absence of such a chelation due to the five-coordinate nature of the complex.

We conclude that model **2** studied in this investigation is presently the best model complex to mimic the activity of HCA. Formation of a bidentate bicarbonate complex inhibits the catalytic cycle. The enzyme may weakly bind to another neighboring group in order to prevent the formation of a bidentate bicarbonate intermediate. Finally, the significant difference in reactivity between the model complexes and HCA may further be due to the ability of the enzyme to stabilize the proton on the coordinated oxygen atom of the bicarbonate intermediate, which can facilitate breakage of both the Zn−O bond during the substitution of HCO_3^- by water and the O−C bond during the release of CO_2 as suggested recently.[11,39]

Acknowledgment. The authors gratefully acknowledge financial support from the Deutsche Forschungsgemeinschaft, the Fonds der Chemischen Industrie, and the Volkswagen-Stiftung.

IC950578N